Open access • Journal Article • DOI:10.1109/JSEN.2015.2425473

Novel Receiver Sensor for Visible Light Communications in Automotive Applications — Source link

Alin-Mihai Cailean, Barthelemy Cagneau, Luc Chassagne, Mihai Dimian ...+1 more authors

Institutions: Ştefan cel Mare University of Suceava

Published on: 22 Apr 2015 - IEEE Sensors Journal (IEEE)

Topics: Visible light communication and Bit error rate

Novel Receiver Sensor for Visible Light Communications in Automotive Applications

Alin Cailean, Barthélemy Cagneau, Luc Chassagne, Mihai Dimian, Valentin Popa

Novel Receiver Sensor for Visible Light Communications in Automotive Applications

Alin-Mihai Cailean, Barthélemy Cagneau, *Luc Chassagne, *Member, IEEE*, Mihai Dimian and Valentin Popa

***Abstract*— This paper presents an easy-to-use sensor aimed for traffic safety applications using visible light communications. A central problem in this area is the design of a suitable sensor able to enhance the conditioning of the signal and to avoid disturbances due to the environmental conditions. The visible light communication sensor proposed in this article addresses these issues and enables a robust communication for short to medium distances. The presentation is focused on hardware aspects and low-level coding techniques. The experimental validation of the proposed sensor has been conducted by analyzing communication performances between a commercial traffic light and the sensor, for distances up to 50 m. The measurements exhibit bit error ratio lower than 10^{-7} in an outdoor configuration, using two well-known codes (Manchester and Miller) without any error-correcting codes or complex signal processing. The prototype is aimed for automotive applications but other outdoor configurations can also be addressed by slight changes in the system design.**

***Index Terms*— infrastructure to vehicle communication, robust sensor, smart lighting systems, vehicle safety applications, visible light communications.**

I. Introduction

DURING the last decade, the semiconductor industry has enhanced performances of light emitting diodes (LED) enabling the development of Visible Light Communications (VLC) systems. An important area of VLC application is the automotive industry where vehicle to vehicle (V2V) and vehicle to infrastructure (V2I or I2V) communications are required to enhance the efficiency and the safety of vehicles in high traffic density which in turn helps to improve traffic regulations and estimations. This includes the transmission of crucial data between vehicles such as information concerning the state of the vehicle (e.g. brake, speed, acceleration, engine failure) or traffic (e.g. state of traffic lights, accidents, traffic jams, line works). The development of the smart transportation infrastructure is an important challenge for the future.

The VLC systems are well suited for V2V and V2I/I2V communications due to their high performance to cost ratio, ease-of-use and the capacity to be developed by using the existing vehicle/infrastructure lighting systems. Recently, significant research effort has been dedicated to the development of communication systems between vehicles and traffic lights [1-6] and even towards the design of large infrastructures, such as Vehicular Ad Hoc Networks (VANETs) with intelligent traffic lights [7]. The main challenges in this area are to increase the rate of the data transfer and to decrease the error rate, as reflected by the recent normative efforts in the intelligent transportation systems such as the IEEE 802.11p [8] and the IEEE 802.15.7 [9] standards.

An example of VLC usage in a highway configuration is illustrated in Fig. 1. Safety vehicles proceed on the damaged cars and transmit the information in the neighborhood of this area. The neighboring cars receive the data by using light sensors and send them further to the next nearest neighbors by using their head/back lights. Data are thus propagated throughout the highway. The traffic infrastructure also contributes to the information broadcast. Furthermore, the cars can also communicate with each other regarding their mechanical state or other issues needed to enhance the traffic safety and the security.

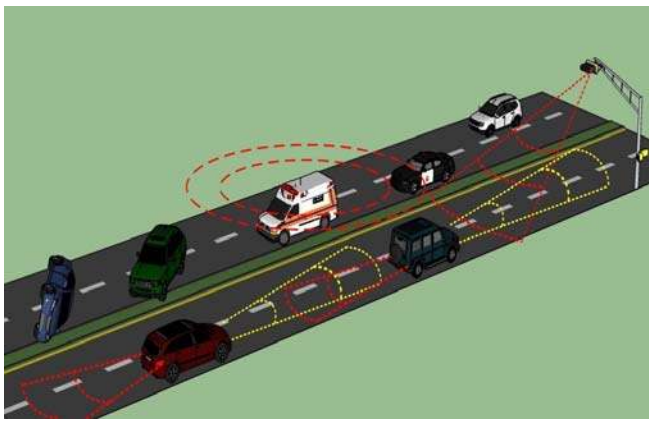

Fig. 1. Illustrations of Visible Light Communication in an outdoor configuration between several vehicles: emergency vehicles alerts users with local broadcast messages and vehicles propagate the information through their lights.

This work was sustained by the competitive cluster Moveo and is partially funded by the national FUI 10 program (project Co-Drive). A.-M. Cailean was supported by the project "Sustainable performance in doctoral and post-doctoral research PERFORM - Contract no. POSDRU/159/1.5/S/ 138963", project co-funded from European Social Fund through Sectorial Operational Program Human Resources 2007-2013.

Alin M. Cailean is with the LISV laboratory of the University of Versailles Saint-Quentin, 10-12 avenue de l'Europe, 78140 Velizy, France and with the Department of Computers, Electronics and Automation of Stefan cel Mare University, Suceava, Romania (e-mail: alinc@eed.usv.ro).

Barthélemy Cagneau and *Luc Chassagne are with the LISV laboratory of the University of Versailles Saint-Quentin, 10-12 avenue de l'Europe, 78140 Velizy, France (corresponding authors phone: +33 1 39 25 49 44; e-mail: {barthelemy.cagneau, luc.chassagne}@ uvsq.fr).

Mihai Dimian and Valentin Popa are with the Department of Computers, Electronics and Automation, Stefan cel Mare University, Suceava, Romania.

This paper is mainly focused on the VLC receiver modules. Based on the fact that the new generation vehicles are already equipped with cameras used for pedestrians and traffic lane detection, it is quite straightforward to use these embedded cameras as VLC receiver modules. However, the automotive industry use relatively low-cost cameras with noise performances lower than the ones of independent photo-elements and which have a limited number of frames per second (fps). Such VLC camera systems can cover distances of 1-2 m with very low data rates [10, 11]. Better results are achieved when high speed cameras are used [12, 13] but they are still too expensive for a broad distribution in automotive industry. On the other hand, photodetectors are quite efficient regarding noise performances and can be used over long distances. However, long range implies active control of the position, which in turn requires the detection of the traffic light. In [14] they achieved this using a low-cost camera. Another possible solution could be the usage of an array of photodiodes along with an adapted beamforming algorithm as the one presented in [15].

In spite of these major research efforts [1-19] and of the advances made in the theoretical developments, the number of VLC prototypes is rather limited as it is the experimental validation in various environmental conditions. In this article, we present a novel sensor module for outdoor VLC applications, focusing on the hardware layer and using low-level coding techniques. Preliminary results of this research have been summarized in [20]. The experimental validation of the proposed VLC sensor is provided, the tests being performed in conditions similar to the ones encountered in the envisioned applications, both outdoor and indoor. The sensing module has been tested for a transmission link using the standard Manchester code as well as the Miller code, suitable for Multi-Input Multi-Output (MIMO) applications as in [21]. The obtained results are very promising taking into account that the BER was lower than 10^{-7} in medium-range communication link under moderate sun exposure without using any error correction codes. With an error-correcting code module based on the Direct Sequence Spread Spectrum (DSSS) techniques such as in [1, 2, 22] or based on pseudo-noise codes, a final BER of 10^{-8}-10^{-9} or even lower can be expected.

II. Design of the Proposed VLC Sensor

The proposed sensor must be able to properly work taking into considerations two major restraints imposed by long range outdoor VLC applications. The first constraint is the limited received power. In this case, the emitted power depends exclusively on the application and on the eye safety norms and thus, increasing the emitted power does not represent an option. The second problem is caused by the ambient interference affecting the link. As demonstrated in [23, 24], the outdoor VLC channel is strongly altered by artificial light sources and by sun radiation. Besides inducing a strong DC component, the background light also represents a strong source of shot noise. Moreover, the intense sunlight can saturate the photoelement and thus block the communication. Therefore, related to these issues, in the development of the proposed sensor, a particular objective was to increase the robustness to noise and to prevent saturation.

A. *Functional block diagram of the receiver sensor*

The proposed sensor is aimed at providing a relatively low-cost solution for a medium range VLC system performing under various environmental conditions. Its functional block diagram is sketched in Fig. 2 and includes an optical collecting system, an electronic front stage for signal reception, an adaptive analog signal conditioning part followed by an analog-to-digital convertor and a signal processing unit. The input signal can be either red or green light sent by a LED traffic light from distances up to 50 m. The optical collecting system is mainly composed of a cover to reduce environmental light coming from the sides and a lens to focus the light on the sensitive part of the photodiode. The resulting reception angle is estimated at ± 10°. A low-cost silicon PIN photodiode with fast response time is used as photodetector and is coupled to a low-cost pre-amplifier in a transimpedance scheme for pre-conditioning the signal. At this level, the gain value is computed in order to prevent photodiode saturation even in direct sun exposure, which has been experimentally verified. When the incident light is within limits that cannot saturate the photosensitive element, the gain is increased. This pre-amplification unit ensures a magnitude level of the input electrical signal on the order of tens millivolts for communication distances up to 50 m. The characteristic bandwidth is lower than 100 kHz but it can be significantly improved, if necessary, by changing the photosensitive element or the operational amplifier. However, the current value is high enough since the rate of transmitted data required in the envisioned road applications is usually lower than 100 kb/s, while the effects of background light noise are thus limited.

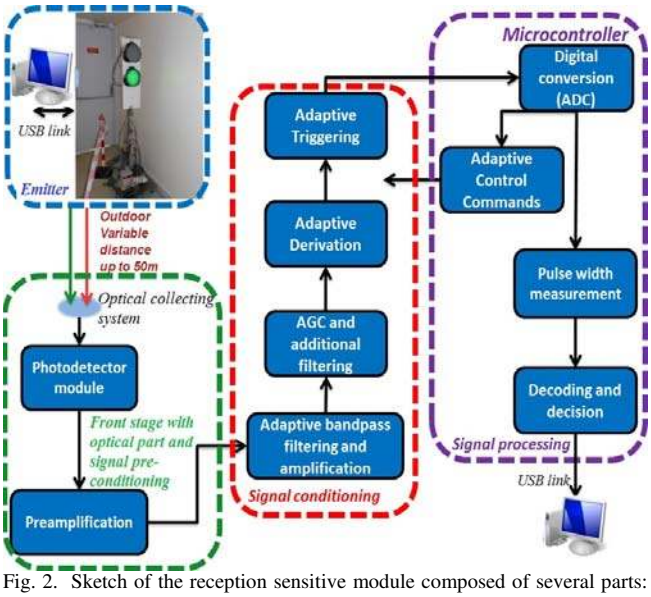

Fig. 2. Sketch of the reception sensitive module composed of several parts: i) optical collecting system, ii) electronic front stage with transimpedance board for signal reception, iii) analog conditioning signal with derivative part, iiii) digital conversion and signal processing with adaptive controls (gain, cutoff frequencies and triggering).

The second stage of the sensor is an analog conditioning board. The analog band-pass filter suppresses the offset due to the daylight or perturbations from artificial light and filters high frequency noise. One of the main parts of the sensor is the adaptive derivation module which amplifies the signal edges and makes the reconstruction process be mainly based on the pulse width rather than the pulse amplitude, as illustrated in Fig. 3. Reconstructing the signal mostly based on the edges and less on the amplitude represents an enhancement which makes the proposed sensor to be less reliant on the power of the incoming signal. This makes it to be suitable for the automotive domain and for other mobile applications in which the emitter – receiver distance fluctuates and thus the received power. The applied signal processing technique is based on the traditional method, still using a band-pass filter. However, in this case the filters are not optimally matched. The optimal matched band-pass filters are indeed effective in rejecting the DC component and also in removing the high frequency shot and thermal noises. Besides removing the noise, such filters also round off the signal edges, outputting a quasi-sinusoidal signal. However, at low signal to noise ratios (SNR), the quality of the resulted sine wave is strongly affected by the intense noise. Furthermore, considering the encoded signal (e.g. using Manchester or Miller codes), depending on the data, pulses of different widths result from the coding. As detailed in sections II B and experimentally illustrated in section III C, the narrow pulse corresponds to a frequency which is twice the one corresponding to the wide pulse. In this case, the filtering has slightly different effects on the different pulse width types. Consequently, the usage of such a signal for the triggering could affect the width of the pulse.

On the other hand, the high-pass filter derivative approach has strong merits. The prototype is aimed to comply for the outdoor environment, where the sunlight represents a major impediment, introducing a high DC component and also a very strong shot noise component. The high-pass derivation efficiently removes the DC noise component. Furthermore, the derivation also allows for precise edge identification. This approach is very efficient at low SNRs because it minimizes the influence of the noise on the pulse width, limiting the distortions. With this method the main objective is to amplify the edges rather than to completely separate the noise from the signal.

Next, the Automatic Gain Control (AGC) unit enables the sensor to properly receive information coming from different distances and SNR. The AGC provides a complementary gain whose value is adjusted according to the input signal power. The AGC stage has as input a DC signal proportional to the amplitude of the previously derived signal. The signal conditioning stage is in connection with the signal processing stage, continuously transmitting information regarding the signal's amplitude. At this level, the sensor includes an analog-to-digital convertor (ADC) and a low-cost 8-bit microcontroller (Microchip 18F2550). Depending on the level of the signal, the microcontroller uses a precise algorithm to select the value of the analog conditioning board. Depending on the amplitude, adaptive gains and complementary filtering are selected.

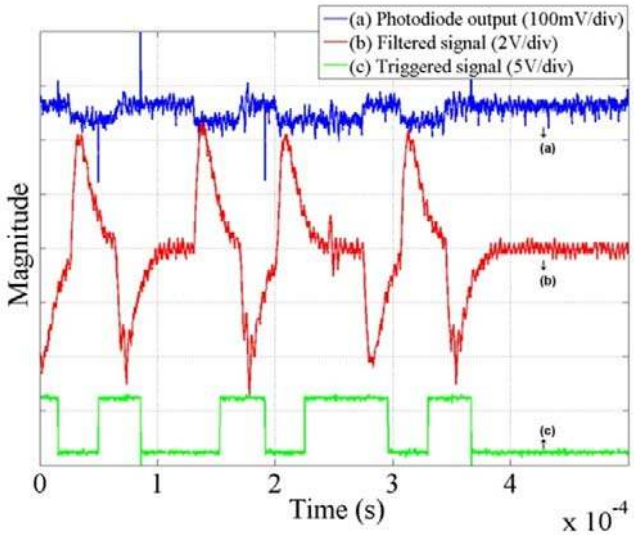

Fig. 3. Example of electric signals on the reception board; a) output of the pre-conditioning board; b) output of the conditioning part and c) output of the decoding and decision block. It illustrates that the derivative part emphasizes the front edges.

Following, the triggering is made based on the previously amplified edges. The resulting signal is transmitted to the main signal processing unit, which performs the message decoding based on the pulse width measurement. The pulse width measurements are performed by the microcontroller, based on a high frequency clock. This process and the decision algorithm are detailed in the experimental part since they are dependent on the codes presented in the next subsection.

B. Discussions about the coding

Two codes have been implemented: the bi-phase Manchester code and the Miller code. The Manchester code's selection is well argued since it is the code specified by the IEEE 802.15.7 standard [9]. According to the standard, the Manchester code is well suited for outdoor low data rate applications, such as the communication between vehicles. Even though the Manchester code has numerous advantages, its bandwidth requirement is larger compared to other codes. Based on this fact, and considering the future demand for MIMO VLC applications, we also have chosen to implement and to investigate the performances of the Miller code. The Miller code can be easily constructed from the Manchester code and has most of Manchester's code advantages. Nevertheless, in addition, the Miller code is also bandwidth efficient, offering the premises for MIMO applications. Furthermore, as detailed in [25], the flickering effect introduced by the Miller code is rather limited, making it safe to be used in outdoor applications. Both codes are used in on-off keying (OOK) configuration and are well suited for short or medium simplex communications where the SNR does not need improvements based on more complex frequency or phase modulation techniques. The OOK modulation is also well adapted to data rates of tens of kilohertz which is sufficient for the envisioned applications.

The Power Spectral Densities (PSD) S_f of these two codes are expressed by eq. 1 and 2, respectively [26]:

$$S_{Man}(f) = V^2T \times \left[\frac{sin^2(\pi fT/2)}{\pi fT/2}\right]^2 \quad (1)$$

$$S_{Mil}(f) = \frac{V^2T}{2(\pi fT)^2[17+8\cos(2\pi fT)]} \times \begin{bmatrix} 23-2cos(\pi fT)-22cos(2\pi fT)-12cos(3\pi fT) \\ +5cos(4\pi fT)+12cos(5\pi fT)+2cos(6\pi fT) \\ -8cos(7\pi fT)+2cos(8\pi fT) \end{bmatrix} \quad (2)$$

where V is the signal magnitude, T the modulation period and f the frequency for which the PSD is calculated.

The corresponding spectra are plotted in Fig. 4a for two selected modulation frequencies. For readability, the curves of the Manchester code have been inverted, so they have negative values. Depending on the amplitude of the signal, the spectra can be scaled by a factor K, which is included, for simplicity, in the PSD unit. It is apparent from Fig. 4a that the Miller code requires a total bandwidth of approximately 12 kHz which is significantly smaller than 27 kHz required by the two channels in the Manchester code. For a five channels simulation of the Miller code, presented in Fig. 4b, one can identify a total bandwidth lower than 150 kHz while the five sub-carriers can be easily filtered by band-pass filters. As a general rule for the Miller code, the PSD is approximately 2/5 of the modulation frequency. These two plots illustrate the Miller code efficiency in channel usage, pointing out its perspectives in future MIMO applications.

In our prototype, the microcontroller can be switched between Manchester and Miller codes in order to test different configurations. The temporal properties of both codes are also important for the detection board in order to design the electronics without using complex decoding algorithms.

The main parameter of the transmission is the width of the elementary moments of the digital bits. For the Manchester code, there are only two symbols (the positive edge and the negative edge) leading to only two combinations of widths: either one elementary bit width or two bit widths. For the Miller code, its memory effect leads to three possible combinations: either one elementary width, or one and a half or two widths [25]. These properties are exploited and detailed in the section III.

C. Description of the transmission test bench

A general VLC test bench has been developed (see Fig. 5), including the receiver previously described and an emitter which can be either a car stop (red) light or a commercial traffic light – switching between red or green lights – with the power modulated by simple digital switches. All the components have been chosen for their low-cost, compactness properties, and for their compatibility with industrial prototypes. The light is current modulated with OOK modulation controlled by a low-cost microcontroller (18F2550 from Microchip) according with the codes mentioned in the previous section. A digital frame has been defined as schematically illustrated in Fig. 5. Several synchronization bits

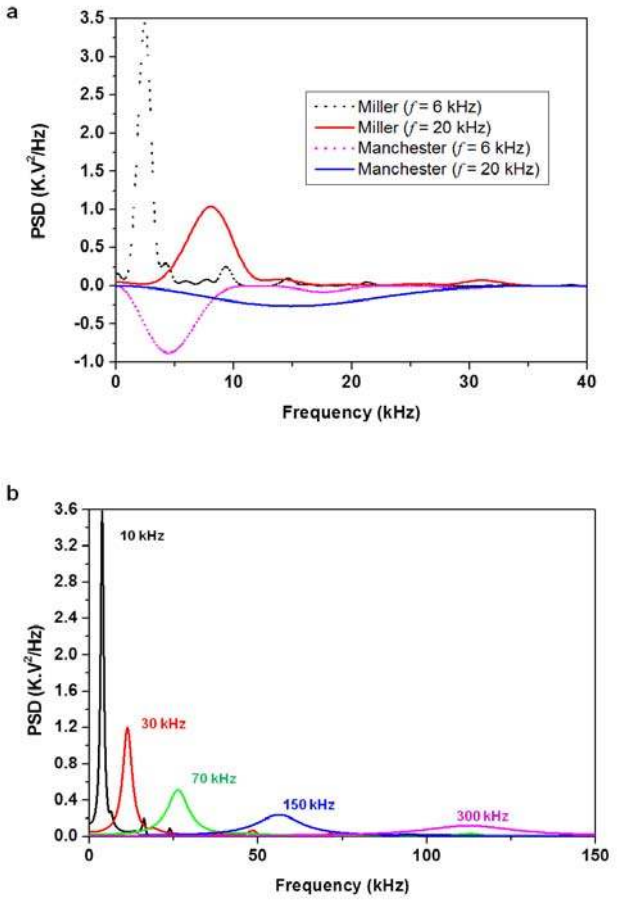

Fig. 4. a) Comparison between Manchester and Miller PSD for two modulation frequencies. Manchester curves are negative for readability; b) Simulation for a five channel configuration with Miller code for modulation frequencies of 10 kHz, 30 kHz, 70 kHz, 150 kHz and 300 kHz. Spectrum separation for Miller code is easier than for Manchester code due to its narrower PSD.

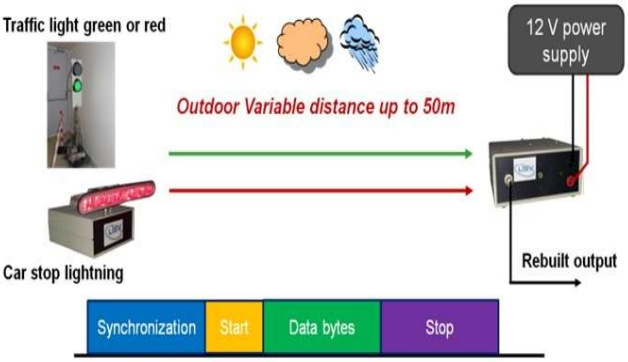

Fig. 5. Sketch of the experimental test bench with the receiver prototype, only supplied by a 12 V battery to be easily embedded. The test emitter can be either a vehicle's red stop lightning, or a commercial traffic light – red or green. The sent data can be Manchester or Miller coded and is composed of a traditional frame with synchronization bits, stat bits, data bytes and stop bits.

begin the frame to alert the receiving board that a message is sent. The rest of the frame is composed of start and stop bits, and an additional flag providing information on the data frame

length. The emitter and receiver are interfaced with a PC through a USB connection and can be placed on a mobile platform which facilitates the variation of the distance between emitter and receiver and their relative directions.

The IEEE 802.15.7 standard for outdoor VLC applications specifies data rates between 11.67 and 100 kb/s in the case of OOK. Since in a first step our main goal is to maximize the communication range and to enhance the robustness to noise, the lowest data rate of the standard was considered. Consequently, the clock of the receiver is not synchronized with phase locked-loop (PLL) for simplicity. However, in order to improve the data rate, the future version of the system should use PLL.

III. Experimental Results and Discussions

The experimental tests have been conducted both indoor and outdoor having as main objective the validation of the VLC prototype under various environmental conditions. The receiver decodes the data in real-time, based on the code information provided in the signal header and proceeds to the post-processing part and to error calculation.

A. *Experiment 1 – Sensitivity determination*

In the first set of experiments, a specific message is sent by using a modulation frequency close to the minimum of the IEEE 802.15.7 standard (11.67 kHz). The noise sensitivity for the pre-conditioning stage of the sensor is illustrated in Fig. 6, where the pure noise spectrum is plotted against the spectra of the detected Miller coded signal for short-range (10 m) indoor communication. A good signal-to-noise ratio and a sensitivity of about – 80 dBm for frequencies above 3 kHz can be observed in these experiments. Since the sensor was developed to work at frequencies close to the lowest one of the standard (11.67 kHz), as the frequency increases above 22 kHz, the sensitivity begins to drop, making the signal amplitude as low as the one of the noise. Within the middle region, the sensitivity for the data signal is high enough. Concerning the noise, it can be observed that its amplitude follows a linear trend for the entire concerned band.

B. *Experiment 2 – Mobility evaluation*

The aim of the second experiment is to test the functionality of the AGC stage. For these experiments, the distance between the emitting traffic light and receiver was changed and the response of the receiver was monitored. While modifying the emitter - receiver distance, the microcontroller computes the gain value in real time and commands its selection on the board. The results illustrating how this value is affected are presented in Fig. 7 for some distances.

One can see how the gain of this stage is amplified with a factor 10 between the shortest and the longest distances. The amplification factor had as purpose to maintain the signal amplitude between the threshold limits. The values of the thresholds were determined experimentally. It was observed that when the signal decreased to half its value, or even below, the signal reconstruction process is not affected. This is possible because, like previously mentioned, the triggering is mainly based on the identification of the rising and of the falling edges rather than the signal's amplitude. This is why, even if the distance decreases 20 times and so the signal's amplitude (at this point), an amplification factor of 10 is sufficient to maintain the signal level within the optimum thresholds.

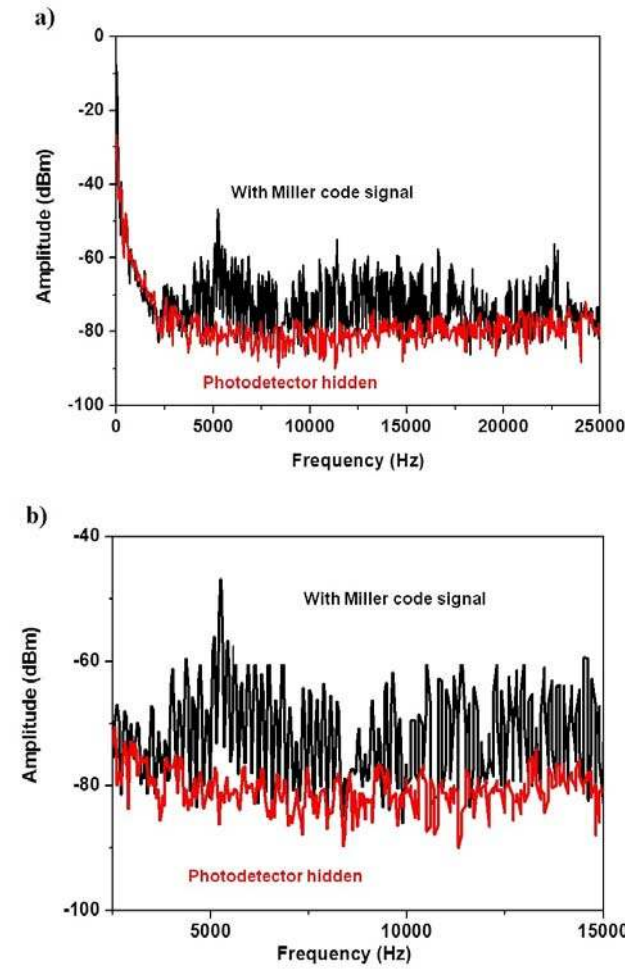

Fig. 6. a) Experiment showing the sensitivity of the front stage of the sensor and example of a spectrum in the case of Miller code; one can see that the signal to noise ratio allows potential detection with low error level ; b) zoom on the central part.

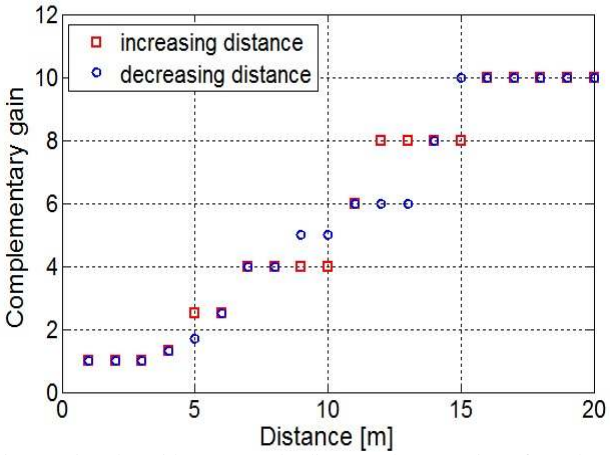

Fig. 7. Gain value with respect to the distance when AGC is performed.

When AGC is performed, the system responds in real time to the variations of the intensity of the incoming signal. This enables the system to maintain a decent BER for the entire length of the service area (SA). The experimental results showed that when the AGC stage is disabled the communication range is reduced if an insufficient gain is preselected. Otherwise, when a high gain is preselected, the system becomes unsuitable at short distances, as in the case when the car is too close to the traffic light, which may lead to the saturation of the sensor.

C. Experiment 3 – Pulse width measurement

In the third set of experiments, the distribution of pulse widths has been analyzed. As mentioned in II *C*, the Manchester code leads statistically to a message composed of two main pulse widths separated by front edges. In our case, the elementary modulation width is approximately 400 microcontroller clock ticks. The accuracy and the stability of microcontroller clock are good enough so the synchronization of the emitter and receiver is not needed. The experimental distributions of the pulse widths are presented in Fig. 8 for approximately 5000 bits sent by using Manchester code (a) and Miller code (b). Two groups of peaks can be observed in Manchester case, one at approximately 400 ticks and another one at approximately 800 ticks. The two groups are divided into two subgroups due to asymmetry of the trigger threshold that generates low-level and high-level triggered values. Although this asymmetry is not necessary, it is a convenient way to distinguish between low-level and high-level values. Since the two groups are apart from each other, the microcontroller is able to count the pulse widths at a high frequency to easily retrieve the digital information. In the case of Miller configuration, three groups of peaks are visible at approximately 800 ticks, 1200 ticks, and 1600 ticks, each group being divided into two subgroups corresponding to low and high levels triggered values. These distributions are useful to adjust the tolerance parameters on the detection threshold for the embedded microcontroller software.

D. Experiment 4 – Bit Error Ratio (BER) determination

A fourth set of experiments has been realized to test the BER. The received bits are compared to the original ones, for sets of data containing 10 million bits obtained by sending repetitively 64 bits. Tests are done either with red light or green light alternatively, generating a BER lower than 10^{-7} which is appropriate for most of the road applications. Additional BER improvement can be obtained by using error detecting codes, correlation techniques or redundancy codes. However, our focus was to evaluate the performance of the sensor. Tests have been realized outdoor and indoor (on a corridor with artificial neon lights generating a strong parasitic 100 Hz signal), the main results being summarized in Table I.

The indoor tests have been made in a corridor, limited to 20 m range because of the limited space available. The aim was to evaluate the robustness of the sensor with respect to neon lights located in the corridor, at a height of 1.5 meters above the receiver. When the light is on, the remaining 100 Hz on

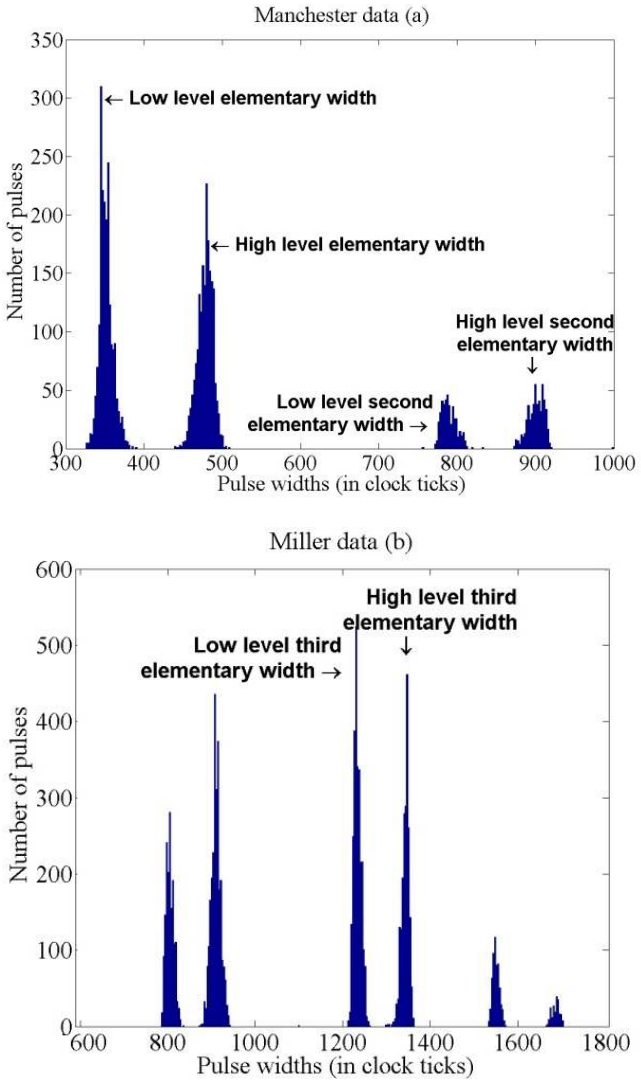

Fig. 8. Histograms of received pulse widths for both Manchester and Miller configurations; a) Manchester case b) Miller case. One can see that the distributions can be easily separated in two groups for the Manchester case (with two sub-groups), and three groups for the Miller case (with each time two sub-groups). Data is plotted with respect to the number of clock ticks. It depends on the microprocessor clock, and can be enhanced with a higher clock frequency.

TABLE I
Bit Error Ratio (BER) for Miller and Manchester codes at 15 kHz modulation frequencies; green and red light have been tested in different conditions.

Code	Conditions	BER
Manchester	1-20 m inside a building with neon light on; Red light	$< 10^{-7}$
	1-36 m outdoor, daylight; Green light	$< 10^{-7}$
	1-50 m outdoor, daylight; Red light	$< 10^{-7}$
Miller	1-20 m inside a building with neon light on; Red light	$< 10^{-7}$
	1-36 m outdoor, daylight; Green light	$< 10^{-7}$
	1-50 m outdoor, daylight; Red light	$< 10^{-7}$

the photodetector module is well filtered and has no influence leading to a BER lower than 10^{-7}. Some errors can appear when the light is switched on or switched off because of transient pulses that can affect the frames but these are minor drawbacks. Both red and green lights show same performances.

The outdoor tests have been performed in different sun exposures, for distances of up to 50 m distance. Within the entire service area, the sensor was able to maintain the BER lower than 10^{-7}, providing a stable communication, which is mainly due to the AGC stage. The front pre-conditioning stage successfully prevented saturation even in the presence of moderate sun.

The sensor shows lower performances for the green light and the associated maximum distance is around 36 m. This is due to three factors: the sensitivity of the photodetector is lower for the wavelength corresponding to the green light than for the red one [23]; the sun spectrum is more disturbing in the green range than in the red one; the used lens is slightly chromatically treated and the transmission coefficient is better for the red light. We plan to enhance this point in the future with higher gain or plastic color filtering to reduce the influence of the sun light and to improve the signal to noise ratio, even for the green light. Finally, note that the traffic lights that we used are commercial ones and not custom-made models unlike in other works [1-5]. In the case of the custom-made traffic lights parameters such light intensity or light emission angle can be adjusted, improving the system performances.

These results demonstrate that the prototype is well suited for data transmission over short or medium distances up to 50 m. Results show 0 errors for 10^7 bits sent for both Manchester and Miller codes. Based on these results, it can also be concluded that the proposed sensor is well suited for applications in which the robustness is more important that data rate, as the vehicular communications.

Unlike in other works, the performances of the system and its suitability for outdoor VLC are confirmed by intensive field testing and not by numerical analysis or simulations. This grants the proposed sensor with increased compatibility with future usage in industrial projects.

IV. Conclusions

This paper presented a very efficient prototype of sensing unit for outdoor visible light communications. The sensor was tested in various conditions in order to verify its reliability in the presence of natural and artificial light. Focusing on the hardware part, the prototype was able to achieve BER results lower than 10^{-7} for distances of up to 50 m. These results are very promising knowing that no error-correcting codes have been used. It must be pointed out that even if there are few other systems similar with the proposed one, this one has the merit of achieving one of the lowest raw BER. Moreover, it is able to maintain the BER at the 10^{-7} level for the entire service area. In this case, the performances of the sensor are limited by the detection sensitivity of the photodiode. This proves that the implemented techniques are well suited even at low SNR. Concerning this issue, it has been experimentally showed that neither the artificial nor the moderate sun, do not affect the communication. The next phase of this research project involves implementing the embedded systems in real road configurations. The optical part was made in cooperation with Valeo industry and is also dedicated to be multi-functions. It was developed to be a vehicle inter-distance sensor as well.

References

[1] N. Kumar, N. Lourenco, D. Terra, L.N. Alves, R.L. Aguiar, "Visible light communications in intelligent transportation systems," *Intelligent Vehicles Symposium (IV), 2012 IEEE* , vol., no., pp.748,753, 3-7 June 2012.

[2] N. Kumar, N. Lourenco, D. Terra, L.N. Alves, R.L. Aguiar "Visible light communication for intelligent transportation in road safety applications," *Wireless Communications and Mobile Computing Conference (IWCMC), 2011 7th International* , vol., no., pp.1513,1518, 4-8 July 2011.

[3] M. Wada, T. Yendo, T. Fujii, M. Tanimoto, "Road-to-vehicle communication using LED traffic light," *Intelligent Vehicles Symposium, 2005. Proceedings. IEEE*, vol., no., pp.601,606, 6-8 June 2005.

[4] T. Saito, S. Haruyama, M. Nakagawa, "A New Tracking Method using Image Sensor and Photo Diode for Visible Light Road-to-Vehicle Communication," *Advanced Communication Technology, 2008. ICACT 2008. 10th International Conference on*, vol.1, no., pp.673,678, 17-20 Feb. 2008.

[5] S. Iwasaki, C. Premachandra, T. Endo, T. Fujii, M. Tanimoto, Y. Kimura, "Visible light road-to-vehicle communication using high-speed camera," *Intelligent Vehicles Symposium, 2008 IEEE*, vol., no., pp.13,18, 4-6 June 2008.

[6] P. Fernandes, U. Nunes, "Platooning with DSRC-based IVC-enabled autonomous vehicles: Adding infrared communications for IVC reliability improvement," *Intelligent Vehicles Symposium (IV), 2012 IEEE* , vol., no., pp.517,522, 3-7 June 2012.

[7] C.T. Barba, M.A. Mateos, P.R. Soto, A.M. Mezher, M.A. Igartua, "Smart city for VANETs using warning messages, traffic statistics and intelligent traffic lights," *Intelligent Vehicles Symposium (IV), 2012 IEEE* , vol., no., pp.902,907, 3-7 June 2012.

[8] IEEE, "IEEE Std 802.11p, Amendment 6: Wireless Access in Vehicular Environements", ed: IEEE, July 2010.

[9] IEEE Standard for Local and Metropolitan Area Networks--Part 15.7: Short-Range Wireless Optical Communication Using Visible Light, "*IEEE Std 802.15.7-2011*, pp.1,309, Sept. 6 2011, doi: 10.1109/IEEESTD.2011.6016195.

[10] C. Danakis, M. Afgani, G. Povey, I. Underwood, H. Haas, "Using a CMOS camera sensor for visible light communication," *Globecom Workshops (GC Wkshps), 2012 IEEE* , vol., no., pp.1244,1248, 3-7 Dec. 2012.

[11] P. Ji, H.-M. Tsai, C. Wang, F.-Q. Liu, "Vehicular Visible Light Communications with LED Taillight and Rolling Shutter Camera," *IEEE Vehicular Technology Conference 2014 Spring*, May 2014.

[12] T. Nagura, T. Yamazato, M. Katayama, T. Yendo, T. Fujii, H. Okada, "Improved Decoding Methods of Visible Light Communication System for ITS Using LED Array and High-Speed Camera," *Vehicular Technology Conference (VTC 2010-Spring), 2010 IEEE 71st* , vol., no., pp.1,5, 16-19 May 2010.

[13] I. Takai, S. Ito, K. Yasutomi, K. Kagawa, M Andoh, S. Kawahito, "LED and CMOS Image Sensor Based Optical Wireless Communication System for Automotive Applications," *Photonics Journal, IEEE* , vol.5, no.5, Oct. 2013, doi: 10.1109/JPHOT.2013.2277881.

[14] S. Okada, T. Yendo, T. Yamazato, T. Fujii, M. Tanimoto, Y. Kimura, "On-vehicle receiver for distant visible light road-to-vehicle communication," *Intelligent Vehicles Symposium, 2009 IEEE* , vol., no., pp.1033,1038, 3-5 June 2009.

[15] A. Lay-Ekuakille, P. Vergallo, D. Saracino, A. Trotta, "Optimizing and Post Processing of a Smart Beamformer for Obstacle Retrieval," *Sensors Journal, IEEE* , vol.12, no.5, pp.1294,1299, May 2012.

[16] C.C. Chang, Y.J. Su; U. Kurokawa, B. I. Choi,, "Interference Rejection Using Filter-Based Sensor Array in VLC Systems," *Sensors Journal, IEEE* , vol.12, no.5, pp.1025,1032, May 2012.

[17] U. Kurokawa, B. I. Choi, C.-C. Chang, “Filter-based miniature spectrometers: Spectrum reconstruction using adaptive regularization,” *IEEE Sensors J.*, vol. 11, no. 7, pp. 1556–1563, Jul. 2011.
[18] S.-H. Yu; O. Shih, H.-M. Tsai; R. Roberts, "Smart automotive lighting for vehicle safety," *Communications Magazine, IEEE*, vol.51, no.12, pp.50,59, December 2013.
[19] Y.-K. Cheong; X.W. Ng; W.-Y. Chung, "Hazardless Biomedical Sensing Data Transmission Using VLC," *Sensors Journal, IEEE*, vol.13, no.9, pp.3347,3348, Sept. 2013.
[20] A. Cailean, B. Cagneau, L. Chassagne, S. Topsu, Y. Alayli, J.-M. Blosseville, "Visible light communications: Application to cooperation between vehicles and road infrastructures," *Intelligent Vehicles Symposium (IV), 2012 IEEE*, pp.1055,1059, 3-7 June 2012.
[21] S.G. Wilson, M. Brandt-Pearce, Q. Cao; J.H., Leveque, "Free-Space Optical MIMO Transmission With Q-ary PPM," *Communications, IEEE Transactions on*, vol.53, no.8, pp.1402,1412, Aug. 2005.
[22] K. Fazel and S. Kasier, “Multi-Carrier and Spread Spectrum Systems”, Wiley, November 2003.
[23] C. Kaiyun, C. Gang, X. Zhengyuan, R.D. Roberts, "Experimental characterization of traffic light to vehicle VLC link performance," *GLOBECOM Workshops (GC Wkshps), 2011 IEEE* , vol., no., pp.808,812, 5-9 Dec. 2011.
[24] C. Kaiyun, C. Gang, X. Zhengyuan, R.D. Roberts, "Line-of-sight visible light communication system design and demonstration," *Communication Systems Networks and Digital Signal Processing (CSNDSP), 2010 7th International Symposium on* , vol., no., pp.621,625, 21-23 July 2010.
[25] A-M. Cailean, B. Cagneau, L. Chassagne, M. Dimian, V. Popa, "Miller code usage in Visible Light Communications under the PHY I layer of the IEEE 802.15.7 standard," *Communications (COMM), 2014 10th International Conference on* , vol., no., pp.1,4, 29-31 May 2014.
[26] The mobile communications handbook, 2nd edition, CRC Press LCC, 1999.

Alin-Mihai Căilean received a B.S. degree in Electrical Engineering (2009) and a M.S. in Computer and Communication Networks (2011) from the University of Suceava (Romania). He received his PhD (2014) after a joint program between the University of Versailles St. Quentin en Yvelines (France) and the University of Suceava (Romania). His main research area is related to visible light communications and wireless sensors.

Luc Chassagne received a B.S. in Electrical Engineering (1994) from Supelec (France) and received his Ph.D. (2000) in optoelectronics from the University of Paris XI, Orsay, (France) for his work in the field of atomic frequency standard metrology. He is now Professor and Director of the LISV laboratory. The topics of interest in his research are nanometrology, precision displacements, sensors and AFM instrumentation.

Barthélemy Cagneau received the Ph.D. degree (2008) in mechanical engineering from the University of Pierre & Marie Curie–Paris 6, Paris (France). After a postdoctoral position in nano-robotics at ISIR (Institut des Systèmes Intelligents et de Robotique, Paris), he became Associate Professor (2009) with the LISV (Laboratoire d’Ingénierie des Systèmes de Versailles, Versailles). His research interests include force control, adaptive control, and robust bilateral couplings for micro- and nano-robotics.

Mihai Dimian received his B.S. in Mathematics (1997) and in Physics (2001), as well as a M.S. in Dynamical Systems from the University of Iassy (Romania). He graduated with a Ph.D. in Electrical Engineering (2005) from the University of Maryland, College Park (USA) and performed post-doctoral research at Max Planck Institute, Leipzig (Germany). He is now full professor and vice-Rector at the University of Suceava (Romania). His research interests are focused on fluctuations and noise in nanoelectronics, stochastic aspects of hysteresis, multiscale analysis and modeling.

Valentin Popa received his B.S. degree in Electronics and Telecommunications (1989) as well as the PhD (1998) from the University of Iassy (Romania). Currently, he is full professor and rector at the University of Suceava (Romania). He is responsible for multiple research grant agreements. His main research areas are: RFID systems, intelligent sensor networks and wireless data transmission systems.